

1N-28
198133
12P

Powdered Aluminum and Oxygen Rocket Propellants: Subscale Combustion Experiments

Mike L. Meyer
*Lewis Research Center
Cleveland, Ohio*

Prepared for the
30th JANNAF Combustion Subcommittee Meeting
sponsored by the Joint Army-Navy-NASA-Air Force Combustion Subcommittee
Monterey, California, November 15-19, 1993



(NASA-TM-106439) POWDERED ALUMINUM
AND OXYGEN ROCKET PROPELLANTS:
SUBSCALE COMBUSTION EXPERIMENTS
(NASA) 12 p

N94-21760

Unclas

G3/28 0198133

POWDERED ALUMINUM AND OXYGEN ROCKET PROPELLANTS: SUBSCALE COMBUSTION EXPERIMENTS

Mike L. Meyer
NASA Lewis Research Center
Cleveland, Ohio 44135

ABSTRACT

Aluminum combined with oxygen has been proposed as a potential lunar in situ propellant for ascent/descent and return missions for future lunar exploration. Engine concepts proposed to use this propellant have not previously been demonstrated, and the impact on performance from combustion and two-phase flow losses could only be estimated. Therefore, combustion tests were performed for aluminum and aluminum/magnesium alloy powders with oxygen in subscale heat-sink rocket engine hardware. The metal powder was pneumatically injected, with a small amount of nitrogen, through the center orifice of a single element O-F-O triplet injector. Gaseous oxygen impinged on the fuel stream. Hot-fire tests of aluminum/oxygen were performed over a mixture ratio range of 0.5 to 3.0, and at a chamber pressure of approximately 480 kPa (70 psia). The theoretical performance of the propellants was analyzed over a mixture ratio range of 0.5 to 5.0. In the theoretical predictions the ideal one-dimensional equilibrium rocket performance was reduced by loss mechanisms including finite rate kinetics, two-dimensional divergence losses, and boundary layer losses. Lower than predicted characteristic velocity and specific impulse performance efficiencies were achieved in the hot-fire tests, and this was attributed to poor mixing of the propellants and two-phase flow effects. Several tests with aluminum/9.8% magnesium alloy powder did not indicate any advantage over the pure aluminum fuel.

INTRODUCTION

Production of propellants from lunar resources has been considered for several decades as a method of reducing the cost of lunar exploration and of providing a lunar base with a level of self sufficiency. More recently, mission analyses have shown significant benefits from using various propellants which can be produced in situ from lunar materials.^{1,2} Although conventional fuel elements such as hydrogen and carbon are scarce at the moon, the ubiquitous lunar regolith can be exploited for propellants. The regolith is composed of oxides of various metals, which can be broken down into the constituent oxygen and metal. This oxygen is an obvious choice for the lunar in situ oxidizer.

The use of in situ oxygen, with a fuel supplied from Earth, can provide significant advantage over a conventional lunar mission scenario, but the benefits of in situ propellants can be improved if the need for an Earth supplied fuel is also eliminated.¹ The metal co-products of oxygen production are the primary candidate lunar fuels. Of these, aluminum shows the most promise.³ It is fairly abundant in the regolith and, when used with liquid oxygen, has the highest theoretical density-impulse of the potential lunar metal/oxygen combinations. However, several known challenges to efficiently using aluminum fuel exist: delivering the fuel to the thrust chamber, completely burning the fuel, and overcoming the effects of condensed material in the exhaust. Without fully understanding the non-ideal performance of an aluminum/oxygen rocket engine, evaluation of its potential benefits to a lunar mission can only be based on estimates of actual performance.

Extensive aluminum fuel literature exists from research on solid propellants which have aluminum added to increase the propellant energy-density. Although this work has not specifically dealt with aluminum/oxygen combustion, it can provide insight into the problems which can be expected with the lunar in situ propellant. Many studies of the combustion of solid propellants have focussed on understanding both the two-phase flow in the exhaust and the metal combustion process. Two-phase flow losses occur in a rocket engine when substances formed during combustion condense in the

chamber or nozzle and then do not maintain thermal or velocity equilibrium with the gaseous combustion products.⁴ This results in a lower momentum flux from the nozzle than would ideally be achieved. Typically, the substances which condense are metal oxides, which will comprise a major portion of the exhaust in an aluminum/oxygen engine.

Incomplete combustion of the metal fuel is also common and can be due to several factors. The fuel particle residence time in the combustion chamber must be sufficiently long for the metal to heat up, vaporize, and combust. In addition, the nature of the aluminum combustion process can cause problems. An excellent overview of the aluminum particle combustion process is provided in reference 5. One key factor to consider is the oxide layer on the fuel particle, which may inhibit combustion and persist even after the drop is liquified and ignited. Alloying magnesium with the aluminum has been proposed to accelerate the particle combustion by creating a more permeable oxide layer. The alloy may also have the advantage of causing disruptive combustion where larger particles breakup into small fragments which burn quickly. Because magnesium is available from the lunar regolith, this concept can also be considered for lunar fuels. Recently, the combustion of various composition aluminum/magnesium alloy particles in hot, high pressure oxygen was studied, and a substantial reduction of ignition delay time was observed for magnesium contents as low as 9.8% by weight.⁶

A more basic engineering problem for an aluminum/oxygen rocket is getting the fuel to the thrust chamber. Several methods have been proposed including liquid metal injection, hybrid rocket designs with a solid fuel grain in the chamber, pneumatic injection of powdered metal, and forming a monopropellant by suspending powdered metal in liquid oxygen.^{1,3} The latter has received the most attention recently, but these studies have focussed on evaluating production and handling hazards and characterizing the thermodynamic properties of the propellant, as opposed to rocket engine performance.^{7,8}

The objectives of the work reported here were to demonstrate a potential propulsion system using aluminum/oxygen propellant, to obtain experimental specific impulse and characteristic velocity data which could be compared to theoretical predictions, and to compare the performance of aluminum/9.8% magnesium alloy fuel to that of pure aluminum. The performance values will be available to guide the assumptions used for lunar in situ propellant mission analyses, resulting in greater confidence in the mission analysis results. In order to accomplish these objectives, both cold-flow evaluation of the fuel feed system and hot-fire engine tests were performed. Pneumatic injection of powdered metal was used for the fuel supply. This method was chosen both to evaluate the technique for transporting metal fuel, and to develop a flexible tool for evaluating the performance of metal/oxygen propellants.

CALCULATIONS

Theoretical characteristic velocity, c^* , and vacuum specific impulse performance calculations for aluminum/oxygen and aluminum/magnesium/oxygen were carried out using the Liquid Propellant Performance Program (LPP)⁹. This program links several modules which predict the performance decrements caused by known loss mechanisms for a liquid propellant rocket engine. These decrements are then used to reduce the ideal performance calculated by the One-Dimensional Equilibrium (ODE) chemistry module. The One-Dimensional Kinetics (ODK) module predicts the performance loss due to finite rate chemistry in the nozzle, and the Two-Dimensional Kinetics (TDK) module calculates losses due to two-dimensional flow and divergence at the nozzle exit. Finally, the Boundary Layer Module (BLM) predicts the losses due to the development of a boundary layer along the chamber and nozzle surfaces. After the boundary layer is calculated, the TDK module is repeated with the wall geometry adjusted by the boundary layer displacement thickness. This then provides a final predicted specific impulse. The LPP program does not have the ability to model the losses associated with condensed species in the exhaust, and in fact, it was not able to converge on a solution for the lower mixture ratio test cases where the mass fraction of condensed phase species became large.

APPARATUS

The hot-fire experiments were performed in Cell 21 of the Rocket Lab at the NASA Lewis Research Center. This test cell is equipped with a 445 N (100 lbf) thrust stand and supporting propellant systems. To accommodate the tests, a powder fuel feed system (figure 1) was added to the facility. The system consisted of a powder filled hydraulic accumulator to store the fuel, a linear displacement transducer to measure the piston motion, and either cold-flow or hot-fire test equipment.

FUEL FEED SYSTEM

A fuel feed system was developed, with a design based on the piston-type positive expulsion fluidized bed concept described in reference 10. The powder fuel was stored in a modified hydraulic cylinder (figure 2) and compressed into the end cap region by the piston. The interstitial voids between the powder particles were pressurized with gaseous nitrogen (GN₂). Upon opening the run valve, the escaping gas entrained the powder from the cylinder and carried it through feed lines to the injector. During a run, the piston continuously compressed the receding powder to prevent undesirable voids from forming. In this manner, a dense stream of powder and gas was created, requiring less than 1% carrier gas by weight to mobilize and transport the fuel. The small gas flow rate was desirable because it allowed the system to be operated in a blow-down mode, without significantly effecting system pressures. It also reduced the overall amount of carrier gas that would be required from Earth for an actual engine in comparison to conventional pneumatic transportation systems which use ~5% carrier gas.

Significant modifications were made to the 6.35 cm (2.5") bore by 45.72 cm (18") stroke hydraulic cylinder to adapt it to the fluidized powder application. The piston rod was rifle-drilled completely through to deliver gaseous nitrogen to the piston. Internal passages in the piston distributed this nitrogen to six carrier gas supply ports. Each of these supply ports was capped with a sintered bronze pneumatic exhaust muffler. The mufflers prevented the powder from working back into the carrier gas lines and facilitated uniform, low velocity injection of the carrier gas. Internal passages were also drilled in the cylinder cap to distribute GN₂ to another set of four carrier gas supply ports near the powder exit port. A pressure tap was also provided in the cylinder cap. The interior surface of the cylinder was plated with a mechanically straightened and honed chrome coating to protect against erosion by the particles. The piston was fitted with two polyurethane U-cup seals, and an additional homogenous nitrile (Buna-N) piston cup was attached to the leading edge of the piston to clean most of the powder from the cylinder wall prior to passage of the seals. This minimized wear on the seals.

A 3/4" pipe run-tee was attached to the powder exit port of the cylinder cap and was large enough to easily fill the piston with a charge of powder by removing a plug from the run of the tee. The branch of the tee was reduced to 1/4" tubing for the fuel line. A standard 1/4" ball valve with reinforced teflon seats provided on/off fuel flow control. In the cold flow setup, the powder line ran from this run valve to a Coriolis force mass flow meter and then either to an injector for spray visualization or to a continuously weighed collection container for gravimetric mass flow measurement. For the hot-fire setup, no Coriolis force flowmeter was used, and the run valve was placed as near to the injector as possible to minimize the start-up transient which occurred while filling the line volume between the valve and injector with fuel.

TEST ENGINE HARDWARE

A sketch of the test engine hardware used for these tests is also shown in figure 1. The hardware consisted of a stainless steel injector body, a 5.23 cm (2.055 inch) inside diameter copper heat-sink thrust chamber, and a copper heat-sink conical inlet conical exit nozzle with a 1.14 cm (0.45 inch) diameter throat, a contraction ratio of 20.85:1, and an expansion ratio of 1.91:1. The heat capacity of the engine allowed several seconds of uncooled firing, which was sufficient to reach steady-state. Two single element impinging injector bodies were fabricated: one O-F-O triplet and one quadlet pattern

with like opposing doublets of fuel and oxygen. Each was equipped with removable injection orifices. This allowed a change of injection area to accommodate the different test conditions without changing the entire injector. Ignition was accomplished with an oxygen/hydrogen augmented spark igniter.

POWDERS

A critical issue of these tests is the particle shape and size distribution of the test powders. These characteristics affect both the combustion of the fuel and the feed system performance. Specifically, smaller particles ignite and burn more quickly and completely, and would thus be more desirable from a combustion standpoint. However, the pneumatic feed system requires a powder that flows fairly well, and very fine particles do not flow well. As the particle size is decreased, electrostatic and adhesive forces become significant, and the particles cling together. A powder of fine particles usually exhibits cohesiveness like flour rather than smooth flow like sand. Thus, a conflict exists between the combustion and flow requirements. Three aluminum powders were tested with mean particle sizes of 15, 25, and 60 micron mean diameters. To maximize the flow of the powder, only spherically atomized particles were tested (the jagged edges of ground particles catch each other and inhibit flow). The 25 micron mean diameter aluminum powder was determined to be the best compromise between flow and combustion. Aluminum/9.8% magnesium powder of similar size and shape was also obtained.

For the cold flow feed system evaluation, several size distributions of inert spherical glass powders were tested. The range of sizes, and resulting flow characteristics, was chosen to allow evaluation of the effect of powder flow on the fuel feed system.

FEED SYSTEM CALIBRATION

Due to the novelty of the powder fuel feed system, a series of cold-flow tests was undertaken to evaluate the system's ability to provide a steady, controlled flow rate of powder at moderately high pressures. To eliminate the potential for combustion during the cold flow tests, glass powder was used to simulate the aluminum fuel. The glass powder closely simulated the aluminum in both specific gravity and particle geometry. The cold flow tests were also used to evaluate two methods of measuring the powder mass flow rate: Coriolis force flow meters and piston displacement of the powder.

Coriolis force mass flow meters have been used to measure two-phase solid/gas flows, but the total flow rate in those applications was much higher than in these tests. This type of mass flow meter operates by subjecting the powder flow to a rotating reference frame and measuring the effect that the resulting Coriolis force has on the powder/gas flow line. The force is proportional to mass flow rate. Because the specific design of Coriolis force mass flow meters varies tremendously, two different manufacturers' meters were evaluated. One of the meters reduced the line cross-sectional area significantly to increase the bulk velocity, whereas the other changed the line cross-sectional area only slightly. Both meters divided the flow into two parallel tubes. The meter which significantly reduced line area caused a large pressure drop and also induced unsteadiness in the flow. The other meter was erratic in its ability to lock onto the proper reading. Neither flowmeter was acceptable for the hot-fire tests.

The alternative to measuring the powder mass flow directly was to measure the motion of the piston with a linear displacement transducer and multiply the volume rate at which powder was displaced from the piston times its density. For this calculation, the powder tapped density was used. The powder flow rate thus calculated was calibrated gravimetrically by collecting the powder flow in a continuously weighed container. Figure 3 shows a comparison of piston motion to the weighed powder mass.

The second purpose of the cold flow tests was to determine the method of regulating the powder flow rate. Two variables were considered for independent control of the powder flow rate: the carrier gas preset pressure and the differential pressure across the piston. The results of studying these

variables are presented in figures 4 and 5. Figure 4 shows the direct relationship between carrier gas set pressure and powder flow rate. In contrast, figure 5 shows that the powder flow rate is not sensitive to the differential force on the piston. It was necessary, however, to maintain a differential force on the piston large enough to prevent coring of the powder (the formation of voids) near the cylinder exit. For this reason, a differential pressure of 1380 kPa (200 psi) was maintained during the hot-fire tests. These results were in general agreement with those presented in reference 9.

HOT-FIRE TEST PROCEDURE

Prior to each test run, the carrier gas pressure was set to obtain the desired powder flow rate, and the piston driving pressure was set approximately 1380 kPa (200 psi) higher than the carrier gas. The nitrogen supply valves were then closed to operate the accumulator in a blow-down mode. The oxygen was also set to obtain the proper flow rate. During the run, the sequencing of events was critical to avoid slag buildup or hardware damage. The following sequence of operation was found to produce the best results:

1. Fuel line purge on
2. Igniter on
3. Oxygen valve opened
4. Fuel valve opened; fuel line purge off
5. Igniter off; igniter purge on
6. Fuel valve closed; fuel purge on
7. Oxygen valve closed; oxygen purge on

The total length of a typical run was three seconds with between 0.3 and 1.0 second of steady-state combustion. A 0.3 second oxygen lag was used at the end of the run to reduce the amount of unburned fuel which accumulated in the chamber. It was necessary to purge the igniter during the run to prevent fuel or combustion products from building up and plugging the outlet to the chamber. This had the undesirable effect of introducing extra nitrogen into the engine. The total nitrogen mass fraction in the propellants was kept below 4.2% for all of the tests.

In addition to the test hardware instrumentation, pressure transducers and thermocouples were located in the primary and igniter gaseous propellant lines to accurately measure propellant flow rates. Each of the 55 instrumentation channels was sampled and recorded 100 times per second. Before final processing, the data was compressed by averaging every ten data points, resulting in ten averaged data points per second. The values presented here were calculated by averaging the data taken during the steady-state portion of the run. Thus a data point represents an average of 30 - 100 scans of the instrumentation.

RESULTS AND DISCUSSION

Hot-fire tests were conducted with both pure aluminum powder and oxygen and aluminum/9.8% magnesium alloy powder and oxygen. The tests were conducted at a nominal chamber pressure of 480 kPa (70 psia) with a nozzle expansion ratio of 1.91:1, although actual chamber pressure varied from 390-630 kPa (57 to 91 psia) due to variations in performance and propellant flow rates. The theoretical performance values were calculated based on actual chamber pressure and indicate that this range of pressure has little effect on performance. Due to limitations in the injector design, most tests were in an oxygen to fuel mixture ratio range of 0.5 to 3.0. Only one test was completed at a higher mixture ratio (O:F=5.8). The higher mixture ratio required a reduction in the fuel flow, and in repeated attempts at O:F>3, the fuel orifice of the triplet injector plugged before steady-state was attained. The combination of high effective fuel density and low flow rates resulted in too slow an injection velocity to keep the orifice clear. A similar problem occurred at all mixture ratios for the quadlet injector, since the fuel was split between two orifices. In an attempt to alleviate this problem, the fuel orifice diameter was reduced, and although this increased the injection velocity, it worsened the powder

plugging problems. Therefore, all of the tests reported used the triplet injector. Mixture ratio could not be increased with additional oxygen because the oxygen flow rates were near the limits of the test facility.

Both characteristic velocity, c^* , and vacuum specific impulse were calculated for the experiments, and the values are compared to the ideal theoretical prediction from ODE. Table 1 contains the test data for the aluminum and the alloy fuels. The experimental c^* was calculated based on measured chamber pressure and propellant mass flow. The experimental vacuum specific impulse was calculated from the measured thrust (corrected for nozzle base pressure and atmospheric conditions) and propellant flow rates.

Figure 6 shows a comparison of the experimental c^* to the ideal ODE calculated values for both pure aluminum and aluminum/9.8% magnesium alloy powder fuels. Solid symbols are used for the pure metal data and open symbols are used for the alloy data. Clearly the performance was quite poor, achieving a maximum efficiency of 72% at a mixture ratio of 2.3. The experimental results follow the same trend as the theory, but increase much more quickly as mixture ratio increases from 0.5 to 2.3. It is not possible to conclude, however, that 2.3 is the optimum mixture ratio for maximizing experimental c^* . The overall low experimental c^* performance indicates incomplete energy release in the thrust chamber. Figure 6 also shows the results of tests with aluminum/9.8% magnesium fuel. There was no benefit to c^* performance from alloying this amount of magnesium in the aluminum fuel.

The c^* performance predicted by the LPP computer code is compared to the experimental results in figure 7. The LPP code was only able to converge for pure aluminum/oxygen at mixture ratios greater than 1.8. Therefore, only four experimental data points were available for comparison, but the theoretical predictions were extended to a mixture ratio of 5.0 assuming the same conditions as for the experimental test at a mixture ratio of 3.0. The experimental c^* is much lower than the predicted values. The LPP code accounts for losses in c^* due to finite rate kinetics, two-dimensional flow, and boundary layer growth, but it assumes complete combustion. The low energy release in the chamber is therefore most likely due to incomplete combustion, which could be caused in large part by poor mixing at the relatively crude injector.

The engine specific impulse was also determined during these tests. Figure 8 presents both the experimental specific impulse (converted to vacuum) and the ideal theoretical vacuum specific impulse calculated by ODE. The small magnitude of even the ideal specific impulse is a result of the small expansion ratio used for these tests ($\epsilon = 1.91$). Again, the experimental performance is poor ranging from 48-68% of the ideal values. Using the aluminum/9.8% magnesium alloy as fuel did not improve specific impulse performance. It is interesting to note that the experimental specific impulse appears to be increasing at an O:F=3.0, indicating a peak above this value, which differs from the ODE predicted peak location near O:F=2.3.

To investigate the cause of the poor specific impulse performance, the LPP predicted values are plotted in figure 9 along with the corresponding experimental results. The theoretical results are again extended to a mixture ratio of 5.0. The code predicts small losses due to finite rate kinetics and two-dimensional effects. A fairly large loss is attributed to the boundary layer in this small engine. However, there is still a large gap between the TDK/BLM and experimental vacuum specific impulse values. As expected, the gap is narrowed significantly if the TDK/BLM predicted values are adjusted for the experimental c^* losses not predicted by the LPP. The adjusted value is obtained by multiplying the TDK/BLM specific impulse by the ratio of experimental c^* to the TDK/BLM c^* . Because the two-phase flow losses have not been accounted for, the experimental specific impulse is still lower than the adjusted vacuum specific impulse. Figure 9 thus indicates that the most significant loss in these tests is the poor c^* performance.

CONCLUSIONS

A system for testing powdered metal/gaseous oxygen propellants in subscale rocket engine hardware was developed and demonstrated. The fluidized powder piston feed system is a viable method of delivering metal fuel to the engine, but an improved injector design is necessary to expand the system mixture ratio capability.

Hot-fire tests for aluminum/oxygen and aluminum/9.8% magnesium/oxygen were completed and performance parameters measured. Both the characteristic velocity and vacuum specific impulse were significantly below predicted values (72% and 68% respective maximum efficiencies). It was shown that the major performance loss was an incomplete release of combustion energy. It was postulated that the incomplete release of energy is due to poor mixing at the injector.

The experimental characteristic velocity and specific impulse increased rapidly with mixture ratio from O:F=0.5. A peak in specific impulse was indicated above a mixture ratio of three. This differs from the ideal calculations which indicate the peak specific impulse occurs at a mixture ratio of about 2.3.

Tests were conducted with aluminum/9.8% magnesium alloy fuel to evaluate the ability of the alloy to improve performance. Neither characteristic velocity or specific impulse were significantly better for the alloy than the pure aluminum fuel.

REFERENCES

1. Wickman, J. H., Oberth, A. E., and Mockenhaupt, J. D., "Lunar Base Spacecraft Propulsion with Lunar Propellants," Paper AIAA-86-1763, AIAA/ASME/SAE/ASEE 22nd Joint Propulsion Conference, June 16-18, 1986.
2. Stancati, M. L., Jacobs, M. K., Cole, K. J., and Collins, J. T., "In Situ Propellant Production: Alternatives for Mars Exploration," NASA CR 187192, October, 1991.
3. Meyer, M. L., "Design Issues for Lunar In Situ Aluminum/Oxygen Propellant Rocket Engines," NASA TM 105433, Paper AIAA-92-1185, AIAA Aerospace Design Conference, February 3-6, 1992.
4. Sarner, S. F., Propellant Chemistry, Reinhold Publishing Corporation, New York, pp. 123-135, 1966.
5. Price, E. W., "Combustion of Metallized Propellants," In Fundamentals of Solid Propellant Combustion, Progress in Astronautics and Aeronautics Series (K. K. Kuo and M. Summerfield, Eds.), AIAA, New York, Vol. 90, pp. 479-514, 1984.
6. Burton, R. L., Roberts, T. A., and Krier, H., "Ignition and Combustion of Lunar Propellants," Final Report for Grant No. NAG 3-1184, University of Illinois Report No. UIUL 93-0504, April, 1993.
7. Woods, S. S., "Liquid-Oxygen/Metal Gelled Propellant Hazards (Phase I)," NASA TR-625-001, NASA JSC White Sands Test Facility, January, 1990.
8. Wickman, J. H., "Liquid Oxygen/Metal Gelled Monopropellants," NASA-CR-187193, October, 1991.
9. Nickerson, G. R., Coats, D. E., Dang, A. L., Dunn, S. S., and Kehtarnavaz, H., "Two-Dimensional Kinetics (TDK) Nozzle Performance Computer Program," NAS8-36863, March, 1989.
10. Loftus, H. J., Montanino, L. N., and Bryndle, R. C., "Powder Rocket Feasibility Evaluation," Paper AIAA 72-1162, AIAA/SAE 8th Joint Propulsion Specialist Conference, November 29-December 1, 1972.

Table 1. Experimental Hot-Fire Test Results

[Al/O₂]

Reading	Mixture Ratio	IVX ^a (sec)	IVAC ^b (sec)	CSX ^c (m/sec)	CSTAR ^d (m/sec)	Pc ^e (kPa)	%N ₂ ^f
65	3.01	131.9	194.0	925.4	1303.3	392.3	4.2
71	1.85	118.8	195.3	831.5	1310.9	412.3	3.7
80	2.15	125.8	196.0	924.2	1316.4	434.4	3.8
85	2.34	123.3	196.2	944.6	1318.0	499.9	3.4
86	1.16	88.3	188.0	658.4	1261.9	450.9	2.8
88	1.43	105.8	191.7	762.6	1286.6	528.8	2.7

[Al/9.8% Mg/O₂]

Reading	Mixture Ratio	IVX ^a (sec)	IVAC ^b (sec)	CSX ^c (m/sec)	CSTAR ^d (m/sec)	Pc ^e (kPa)	% N ₂ ^f
126	0.69	84.9	180.5	520.0	1211.6	411.6	2.5
127	0.61	82.1	178.4	558.6	1196.9	466.1	2.4
128	1.88	110.2	195.7	890.9	1314.0	619.1	2.7
129	1.11	96.9	189.7	733.7	1273.1	624.7	2.3
130	5.79	123.7	180.8	944.0	1216.2	592.9	2.9

- a vacuum specific impulse, experimental
- b vacuum specific impulse, ODE
- c characteristic velocity, experimental
- d characteristic velocity, ODE
- e thrust chamber pressure
- f % nitrogen as a fraction of the total propellant

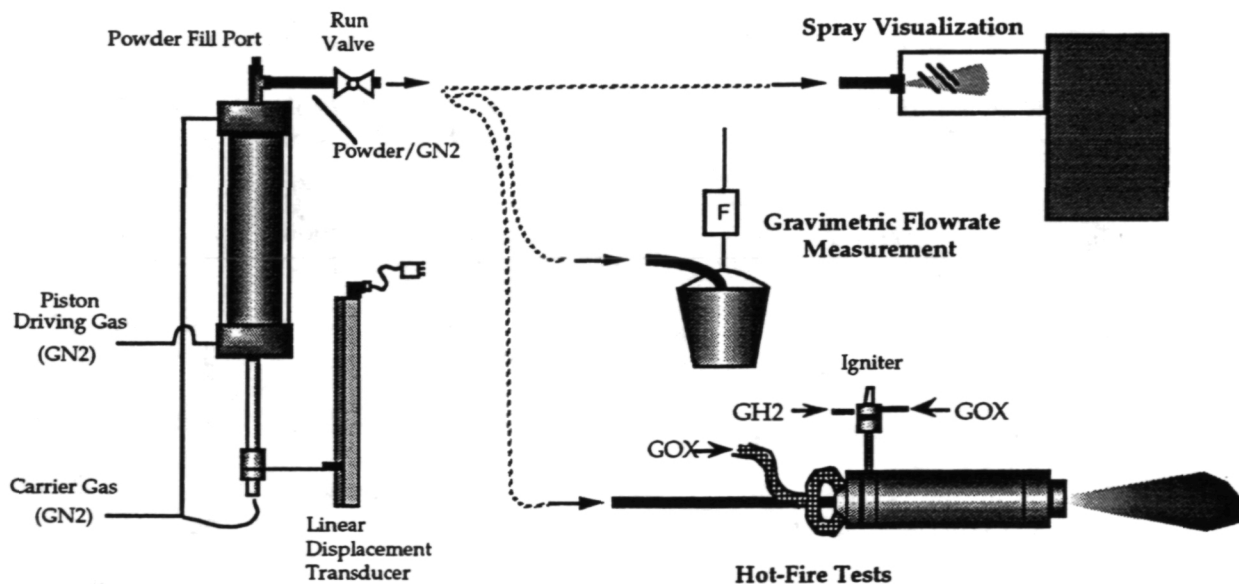


Figure 1. Major components of the cold-flow and hot-fire test rigs.

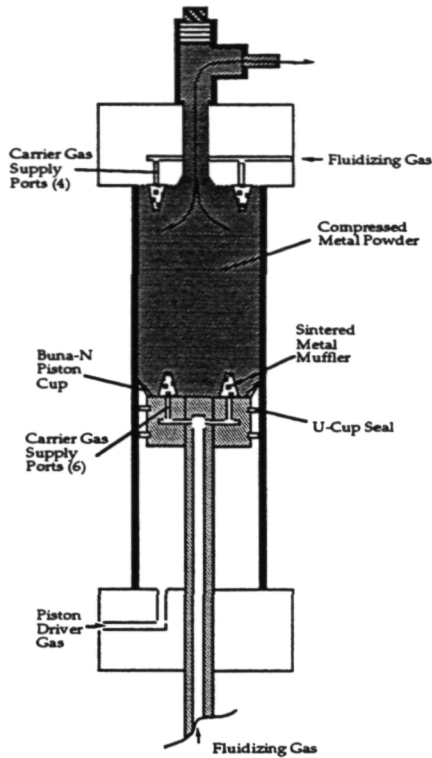


Figure 2. Cutaway sketch of the piston powder feed system.

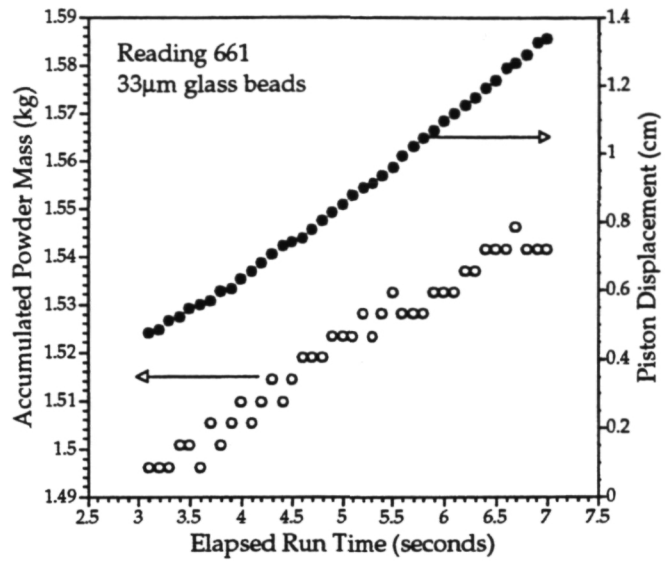


Figure 3. Comparison of accumulated powder mass to piston motion during a representative gravimetric calibration test.

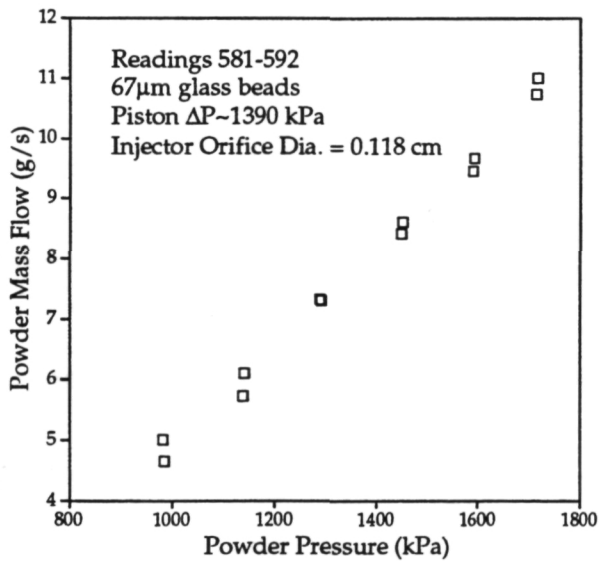


Figure 4. The dependence of powder mass flow rate on the powder carrier gas set pressure.

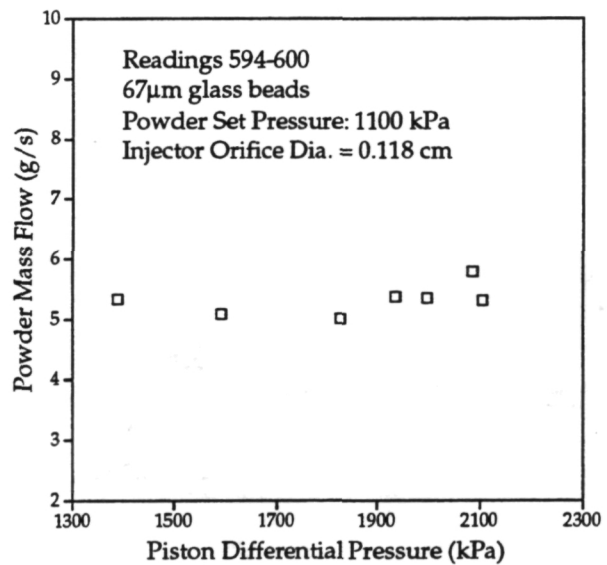


Figure 5. The effect of piston differential pressure on powder mass flow.

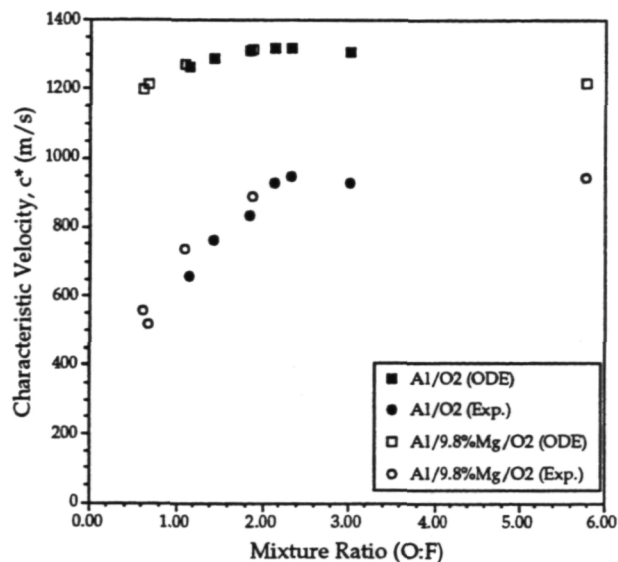


Figure 6. Comparison of the experimental and ideal theoretical (ODE) characteristic velocity of aluminum/oxygen and aluminum/9.8% magnesium/oxygen at ~480 kPa (70 psia).

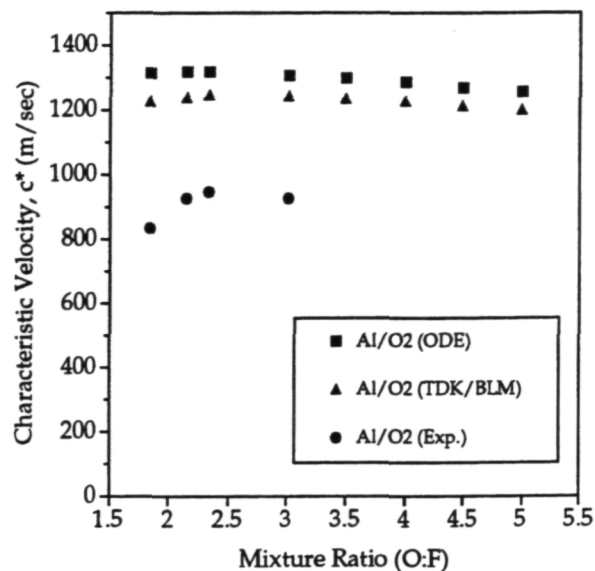


Figure 7. Experimental and LPP predicted characteristic velocity for aluminum/oxygen at ~480 kPa (70 psia).

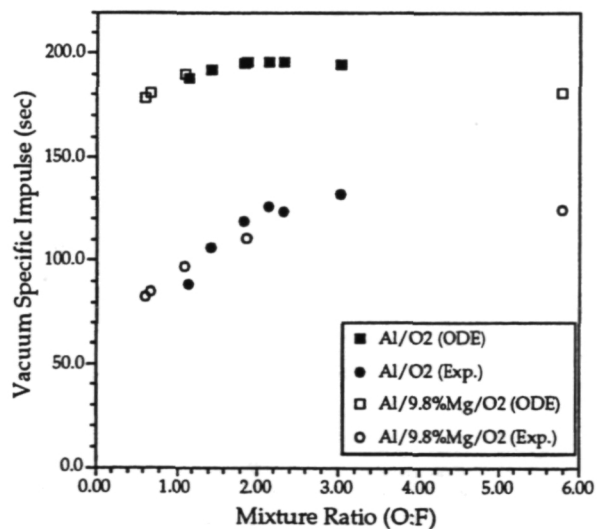


Figure 8. Experimental and ideal theoretical (ODE) vacuum specific impulse for aluminum/oxygen and aluminum/9.8% magnesium/oxygen at ~480 kPa (70 psia).

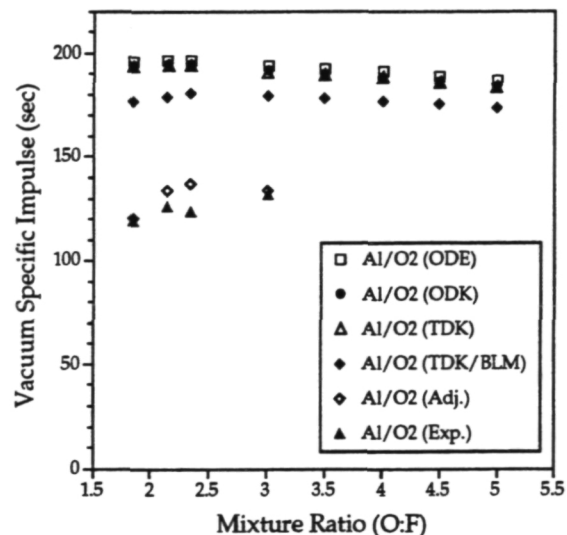


Figure 9. Experimental and LPP predicted vacuum specific impulse for aluminum/oxygen at ~480 kPa (70 psia).

REPORT DOCUMENTATION PAGE

Form Approved
OMB No. 0704-0188

Public reporting burden for this collection of information is estimated to average 1 hour per response, including the time for reviewing instructions, searching existing data sources, gathering and maintaining the data needed, and completing and reviewing the collection of information. Send comments regarding this burden estimate or any other aspect of this collection of information, including suggestions for reducing this burden, to Washington Headquarters Services, Directorate for Information Operations and Reports, 1215 Jefferson Davis Highway, Suite 1204, Arlington, VA 22202-4302, and to the Office of Management and Budget, Paperwork Reduction Project (0704-0188), Washington, DC 20503.

1. AGENCY USE ONLY (Leave blank)		2. REPORT DATE December 1993	3. REPORT TYPE AND DATES COVERED Technical Memorandum	
4. TITLE AND SUBTITLE Powdered Aluminum and Oxygen Rocket Propellants: Subscale Combustion Experiments			5. FUNDING NUMBERS WU-232-01-OA	
6. AUTHOR(S) Mike L. Meyer				
7. PERFORMING ORGANIZATION NAME(S) AND ADDRESS(ES) National Aeronautics and Space Administration Lewis Research Center Cleveland, Ohio 44135-3191			8. PERFORMING ORGANIZATION REPORT NUMBER E-8281	
9. SPONSORING/MONITORING AGENCY NAME(S) AND ADDRESS(ES) National Aeronautics and Space Administration Washington, D.C. 20546-0001			10. SPONSORING/MONITORING AGENCY REPORT NUMBER NASA TM-106439	
11. SUPPLEMENTARY NOTES Prepared for the 30th JANNAF Combustion Subcommittee Meeting sponsored by the Joint Army-Navy-NASA-Air Force Combustion Subcommittee, Monterey, California, November 15-19, 1993. Responsible person, Mike L. Meyer, (216) 433-7492.				
12a. DISTRIBUTION/AVAILABILITY STATEMENT Unclassified - Unlimited Subject Category 28			12b. DISTRIBUTION CODE	
13. ABSTRACT (Maximum 200 words) Aluminum combined with oxygen has been proposed as a potential lunar in situ propellant for ascent/descent and return missions for future lunar exploration. Engine concepts proposed to use this propellant have not previously been demonstrated, and the impact on performance from combustion and two-phase flow losses could only be estimated. Therefore, combustion tests were performed for aluminum and aluminum/magnesium alloy powders with oxygen in subscale heat-sink rocket engine hardware. The metal powder was pneumatically injected, with a small amount of nitrogen, through the center orifice of a single element O-F-O triplet injector. Gaseous oxygen impinged on the fuel stream. Hot-fire tests of aluminum/oxygen were performed over a mixture ratio range of 0.5 to 3.0, and at a chamber pressure of approximately 480 kPa (70 psia). The theoretical performance of the propellants was analyzed over a mixture ratio range of 0.5 to 5.0. In the theoretical predictions the ideal one-dimensional equilibrium rocket performance was reduced by loss mechanisms including finite rate kinetics, two-dimensional divergence losses, and boundary layer losses. Lower than predicted characteristic velocity and specific impulse performance efficiencies were achieved in the hot-fire tests, and this was attributed to poor mixing of the propellants and two-phase flow effects. Several tests with aluminum/9.8% magnesium alloy powder did not indicate any advantage over the pure aluminum fuel.				
14. SUBJECT TERMS Aluminum; Powdered aluminum; Aluminum alloys; Combustion; Extraterrestrial resources; Lunar exploration; Metal fuels; Two-Phase flow			15. NUMBER OF PAGES 12	
			16. PRICE CODE A03	
17. SECURITY CLASSIFICATION OF REPORT Unclassified	18. SECURITY CLASSIFICATION OF THIS PAGE Unclassified	19. SECURITY CLASSIFICATION OF ABSTRACT Unclassified	20. LIMITATION OF ABSTRACT	

National Aeronautics and
Space Administration

Lewis Research Center
21000 Brookpark Rd.
Cleveland, OH 44135-3191

Official Business
Penalty for Private Use \$300

POSTMASTER: If Undeliverable — Do Not Return